Single-Phase Modeling in Microchannel with Piranha Pin Fin

Xiangfei YU[*1], Corey Woodcock[1], Yoav Peles[2], Joel Plawsky [1]
1. Rensselaer Polytechnic Institute, Mechanical, Aerospace, and Nuclear Engineering, 110 8th St, Troy, NY 12180
2. University of Central Florida, Mechanical and Aerospace Engineering, 4000 Central Florida Blvd, Orlando, FL 32816
*yux2@rpi.edu

Abstract: In this paper, a novel pin fin design named Piranha Pin Fin (*PPF*) is proposed to enhance heat transfer in microchannel. More heat transfer area can be obtained by adding pin fins in microchannel. At the same time, this *PPF* realizes vapor venting when fluid is heated to reach boiling temperature. So this design can be applied to either single-phase flow or two-phase flow in microchannel. In this study, silicon based microchannel with *PPF* arrays has been fabricated and tested. For single-phase flow, the key parameters for evaluating the performance of this design have been recorded and analyzed. To validate the experimental data, a 3D model with physics of conjugate heat transfer and laminar flow has been built with COMSOL. The validated single-phase data provides important fundamentals for further research on optimization of the *PPF* design and flow boiling phenomenon.

Keywords: Piranha Pin Fin, microchannel heat transfer, COMSOL simulation

1. Introduction

Microchannel has been extensively studied as it shows potential to meet the cooling requirement for intensive heat input system. Besides weight load reduced, microchannel is capable of enhancing heat transfer based on the small-scale effect. Single-phase fluid flow in microchannel was first studied in 1981 by Tuckerman and Pease [1]. At that time, the highest heat flux they achieved was 790 W/cm^2 with water. Maximum substrate temperature rise was 71℃ above the input water temperature. After this, researchers put effort to implement different design in microchannel [2-4]. In the following decade, fundamental studies were emphasized. It was mainly about validation of continuum theory for incompressible fluid flow in microchannels [5, 6]. In recent years, with the increasing demand for dissipating high heat flux in MEMS and other system, more attention has been paid to heat transfer enhancement. Adding pin fin in microchannel is an effective way to enhance heat transfer between hot surface and cold fluid. Kosar and Peles [7] performed a study on thermal and hydraulic study of MEMS-based pin fin heat sink. DI water was used as working fluid, and a bank of shrouded staggered micro pin fins is etched into the microchannel. The pin fins were 243 μm long with hydraulic diameter equal of 99.5 μm. Heat flux ranged from 3.8 W/cm^2 to 167 W/cm^2 and Reynolds number ranged from 14 to 112. Also, a comparison between experimental data and long tube correlations was made.

Colgan et al. [8] reported a silicon microchannel cooler with optimized fin designs for high power chips. This cooler should be capable to dissipate power density of 400 W/cm^2. And the pressure was smaller than 35 kPa. And the temperature difference between chip's average temperature and fluid inlet temperature can be up to 35°C or even higher.

Xu et al. [9] designed a heat sink which composed of parallel longitudinal microchannels and transverse microchannels. The idea was to separate the whole flow length into independent zones. By doing this, the heat transfer was enhanced and the pressure drop decreases.

In this paper we proposed a novel pin fin, it's named Piranha Pin Fin shown as Fig. 1. With adding these pin fins in microchannel, the heat transfer area is increased. At the same time, pin fin can disturb the fluid flow and enhance the heat transfer further. Also, the chimney in the body of *PPF* can realize extraction or injection of working fluid based on operation conditions. Furthermore, in consideration of dissipating even higher heat flux, this device can be utilized in flow boiling region and *PPF* chimney is designed to vent vapor. In this way, flow boiling heat transfer can be enhanced. For the following parts, the experimental set up and COMSOL simulation will be discussed in detail. A good

match from experimental and numerical has been obtained.

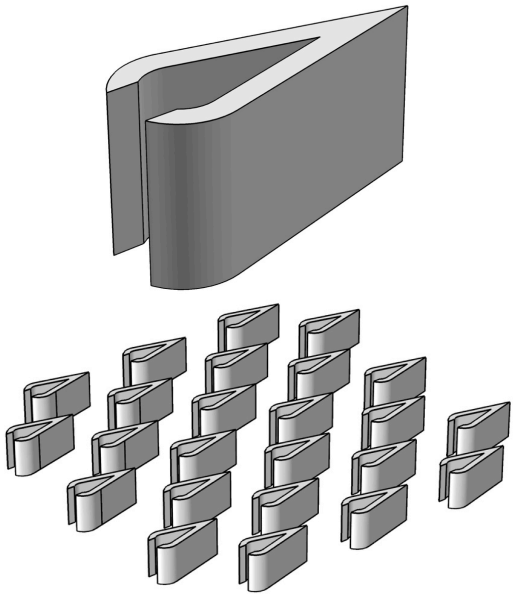

Figure 1. Single *PPF* design and *PPF* array

2. Experimental Apparatus & Procedure

Experimental system set up is depicted in Fig.2. The apparatus mainly included three parts, flow measurement, thermal measurement, and data recording. With this system set up, both diabatic and adiabatic tests can be conducted [10].

For fluid flow, helium tank was connected to pressurize tank containing test fluid *HFE7000*. Without turning on the pump, the system was able to hold the same pressure with tank. After micro pump and valves are turned on, fluid came from the tank and flow through the flow meter; as a result, the inlet flow rate can be obtained. As the package has two outlets, so another two flow meters were connected in this loop to test the outlet flow rate separately. At the same time, three pressure transducers were mounted into the loop, with these three pressure transducer, the pressure drop for fluid flowing through the package can be obtained. For thermal measurement, one power supply and two multi-meters were connected to the loop. This was mainly for heat flux measurements and surface temperature measurement. Furthermore, T-type thermal couples were applied to provide the fluid temperature measurement. Signals from pressure transducer and thermal couples were recorded in the desktop with LABVIEW.

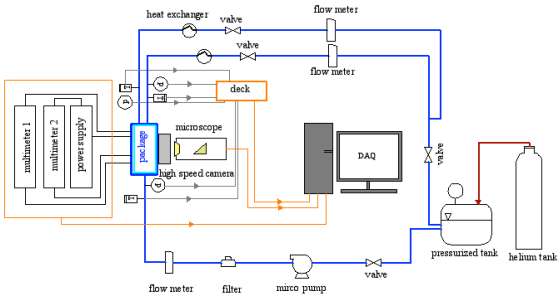

Figure 2. Schematic diagram for apparatus

Figure 3. shows how device was hosted in the package. Cover plate was for applying pressure on the top of the device and holding the system pressure. The silicon device fit in the groove. O-rings were placed underneath the device for inlet and outlet sealing. At the bottom, probes were fixed and contacted with the heaters contact pad for average surface temperature measurements.

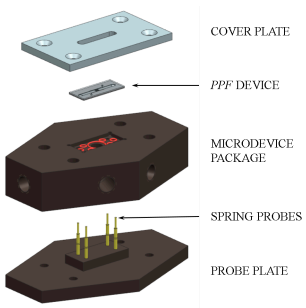

Figure 3. Exploded diagram for test package

In terms of designed device dimension, they are shown in Fig. 4. For a single device, we have one inlet and one outlet. At the same time, when fluid flow through *PPF* array, part of the fluid can be extracted by the chimney just as discussed before. A single PPF SEM image is also provided in Fig.4.

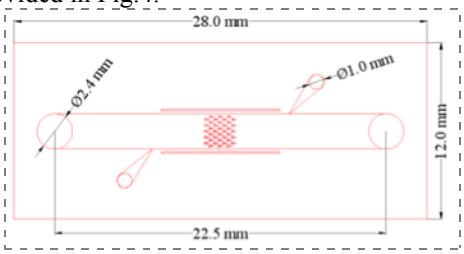

(a) Device dimension

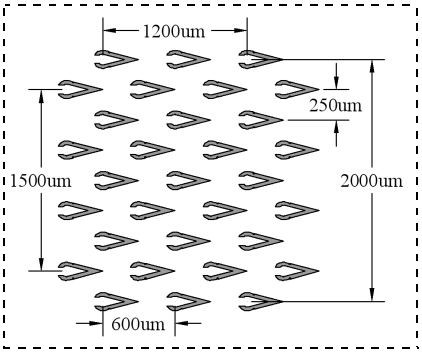

(b) Dimension of *PPF* array

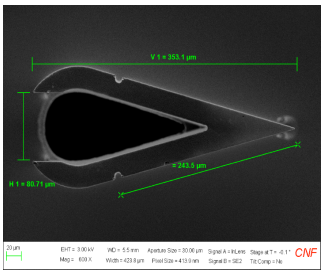

(c) SEM images for single *PPF*

Figure 4. Dimensions and SEM images for device and PPF arrays

3. Model Development-use of COMSOL Multi-physics

Two main physics are involved in this modeling, they are laminar fluid flow, and solid and fluid heat transfer. The governing equations are shown below including mass continuity as incompressible fluid, momentum conservation and energy conservation. All the cases are run under the stationary state.

$$\rho(u\cdot\nabla)u=\nabla\cdot\left[-pI+\mu\left(\nabla u+(\nabla u)^T\right)-\frac{2}{3}\mu(\nabla\cdot u)I\right]+F$$

$$\nabla\cdot(\rho u)=0$$

$$\rho c_p u\cdot\nabla T+\nabla\cdot q=Q+Q_{ted}$$

$$q=-k\nabla T$$

For conjugate heat transfer, boundary conditions are set as Fig.5. As average surface temperature and pressure drop can be obtained from experiments. The working fluid is HFE 7000, which is not available in build-in library. All the properties needed was input in the software and saved as user-defined fluid. To explicitly illustrate the modeling set up, Fig. 5 shows the solid and liquid component separately.

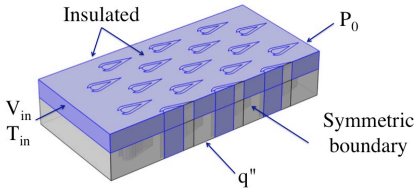

(a) Boundary condition set up

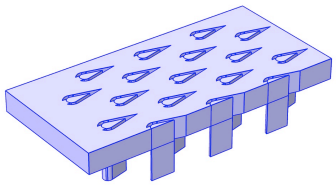

(b) Liquid phase

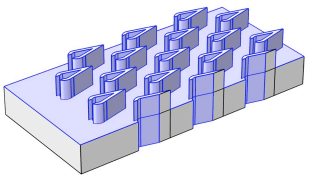

(c) Solid component

Figure 5. Modeling set up

4. Results

The conjugate model is solved in COMSOL. It provides average wall temperature for comparison with experimental data. In terms of pressure drop, to better match the model set up with experimental settings, and adiabatic model was also solved. It contains two section of plain channel from the pressure port to *PPF* array and from the end of *PPF* to pressure port.

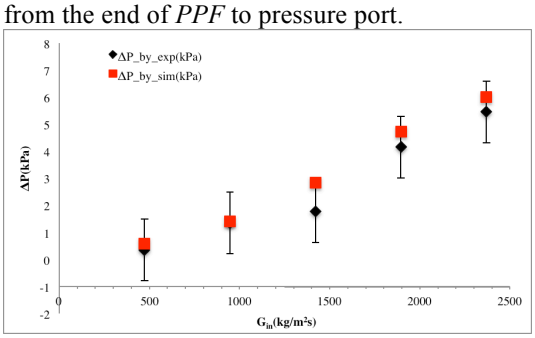

Figure 6. Pressure drop comparison

The pressure drop shown above is defined as the pressure difference measured from upstream and downstream pressure port. G_{in} is the mass flux defined in the channel inlet. Fig. 6 provides pressure drop data obtained from both

experiments and simulations. They match with each other in a good range. The differences are in the experimental uncertainties. Pressure drop increases with mass flux increases as expected.

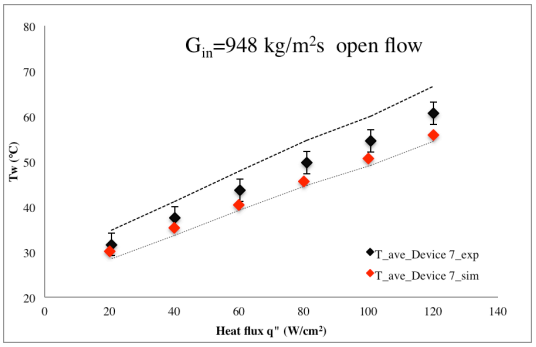

Figure 7. Average surface temperature comparison

For heat transfer part, the model shown in Fig.5 is applied. Mass flux is fixed and heat flux applied through bottom is kept increasing. Average surface temperature increases linearly with heat flux increasing, which implies that heat transfer coefficient rarely changes. This is very reasonable since mass flux is fixed and constant fluid properties are applied.

Figure 8 shows temperature distribution in working fluid and silicon base. As heat flux is applied on the bottom of the microchannel and the sidewalls are in the insulation condition, heat will be removed by the cold fluid in microchannel. At the same time, cold working fluid will be extracted by PPF chimney. As a result, the bottom surface temperature will increase along fluid flow direction. This can be clearly observed from Figure. 8. Furthermore, in vertical direction, silicon base dissipates the applied heat flux well; the temperature gradient is much smaller than that in horizontal direction.

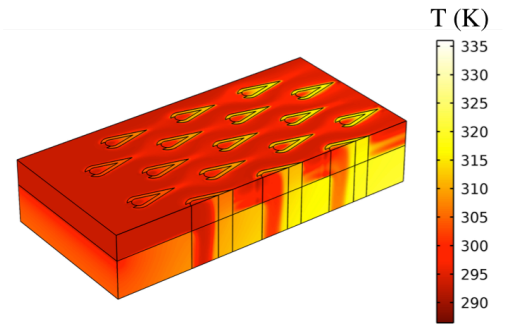

Figure 8. Surface temperature for solid and fluid

Looking into *PPFs* array in microchannel as shown in Fig. 9, in average, the last row of *PPF*'s temperature reaches 330K, which is 25 K higher than that of the first row. In other words, *PPFs* in the first array are well cooled down for facing the cold fluid; however, as the last arrays are shadowed in the wake region, they are not well interacted with cold fluid. Furthermore, zoom in the temperature distribution for single *PPF*, it is found that temperature increases from front to rear and from bottom to the top. Taking the streamline into consideration as shown in Fig. 10, recirculation is formed at the tail of *PPF*. As a result, heat cannot be dissipated effectively and a hot spot site is generated. However, this can be a candidate site for nucleation boiling. Furthermore, if a cavity can be fabricated around the hot spot, nucleation boiling will be initiated.

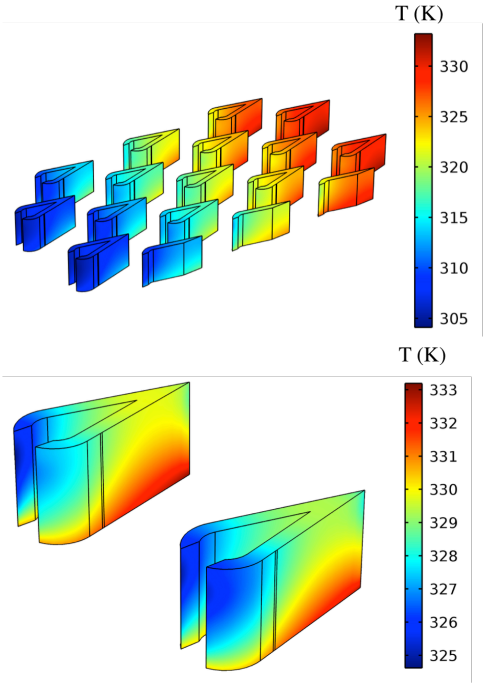

Figure 9. Surface temperature for *PPF* arrays and single *PPF*

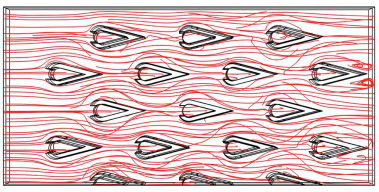

Figure 10. Streamline demonstration

5. Conclusions

In this paper, a microchannel model with conjugated heat transfer and laminar fluid flow is demonstrated. Both hydraulic and thermal characteristic are discussed. Two critical parameters i.e. average surface temperature and pressure drop match the experimental data well. It is also found that PPF is capable to dissipated heat with the working fluid with HFE7000. Furthermore, temperature distribution for silicon base is well analyzed and this provides reference for further flow boiling study.

6. References

1. D. B. Tuckerman and R. F. W. Pease, "High-performance heat sinking for VLSI," IEEE Electron Device Lett., vol. 2, no. 5, pp. 126–129, May 1981.
2. L. J. Missaggia, "ThW.4 Microchannel Heat Sinks and Microlens Arrays for High Average-Power Diode Laser Arrays," pp. 447–449.
3. J. L. Technoi, "DIAMOND-SHAPED INTERRUPTED COOLING FIN FOR HIGH-POWER LSI COMMENT THERMAL MODEL OF LASER DIODE," vol. 23, no. 9, pp. 456–457, 1987.
4. M. F. Catedra, C. Universitaria, J. C. Cruellas, J. F. Diaz, and T. De Ardoz, "Optimal structure for microgrooved cooling fin for high-power lsi devices," vol. 22, no. 25, 1986.
5. J. Judy, D. Maynes, and B. W. Webb, "Characterization of frictional pressure drop for liquid flows through microchannels," Int. J. Heat Mass Transf., vol. 45, no. 17, pp. 3477–3489, Aug. 2002.
6. X. F. Peng, G. P. Peterson, and B. X. Wang, "FRICTIONAL FLOW CHARACTERISTICS OF," no. November, pp. 249–264, 1994.
7. A. Koşar and Y. Peles, "Thermal-Hydraulic Performance of MEMS-based Pin Fin Heat Sink," J. Heat Transfer, vol. 128, no. 2, p. 121, 2006.
8. Colgan, E.G., Furman, B., Gaynes, M., Graham, W., LaBianca, N., Magerlein, J.H., Polastre, R.J., Rothwell, M.B., Bezama, R.J., Choudhary, R., Marston, K., Toy, H., Wakil, J., Zitz, J., and Schmidt, R., 2007, "Practical Implementation of Silicon Microchannel Coolers for High Power Chips", IEEE Transactions on Components and Packaging Technologies, vol. 30, no. 2, pp. 218-225.
9. J. L. Xu, Y. H. Gan, D. C. Zhang, and X. H. Li, "Microscale heat transfer enhancement using thermal boundary layer redeveloping concept," Int. J. Heat Mass Transf., vol. 48, no. 9, pp. 1662–1674, Apr. 2005.
10. Corey Woodcock, Xiangfei Yu, Joel Plawsky, Yoav Peles. "Piranha Pin Fin (PPF) — Advanced flow boiling microstructures with low surface tension dielectric fluids" Int. J. Heat Mass Transf. Volume 90, November 2015, Pages 591–604.

7. Acknowledgements

This research has been funded under the DARPA ICECool fundamentals program. The authors would like to acknowledge the staff in the Cornell Nano-Scale Facility for their assistance in fabrication of the devices.